Gas Rich Dwarfs from the PSS-II I. Catalog and Characteristics

James M. Schombert
Department of Physics, University of Oregon

Rachel A. Pildis
Harvard-Smithsonian Center for Astrophysics

Jo Ann Eder
Arecibo Observatory[1]

ABSTRACT

This project is a visual search for field dwarf galaxies using Second Palomar Sky Survey photographic plates. A morphologically selected sample of 310 objects yielded 145 detections of true dwarfs within a redshift search window of 0 to 10,000 km sec^{-1}. We confirm the low mass, dwarf nature of the same by comparison of luminosity, isophotal size, HI mass and HI profile width distribution of other dwarf samples. The goal of this project is to use these newly discovered dwarf galaxies to map large scale structure as a test of biased galaxy formation. Initial indicators are that the large scale distribution of dwarf galaxies is identical to bright, high mass galaxies, in contradiction to theory using biasing. The full analysis of the sample will be reported in the final paper of our series.

1. Introduction

Dwarf galaxies have received a great deal of observational attention in the last decade for two reasons. The first is that their intrinsic properties provide insight into galaxy formation because dwarf galaxies represent the other extreme in the global galaxy mass distribution. Studying the range of galaxy types from dwarfs to giants is a key test of galaxy formation and evolution models. The second reason deals with the capability of dwarf galaxies to serve as tracers of dark matter. Investigations of dark matter in recent years have questioned the basic premise that light traces the mass on large scales (see Oemler 1988) and there have been suggestions that dwarf, or low mass galaxies, may better sample the distribution of mass in the Universe (Dekel and Rees 1987). The most extreme views question whether the galaxy formation process itself may be biased such that galaxies which formed from low amplitude fluctuations in the early Universe (i.e. dwarf galaxies)

[1]The Arecibo Observatory is part of the National Astronomy and Ionosphere Center which is operated by Cornell University under contract with the National Science Foundation.

are the true indicators of the large scale distribution of mass (Giovanelli, Haynes and Chincarini 1986, Davis and Djorgovski 1985).

The hypothesis that bright, or high mass, galaxies do not trace the true mass distribution of the Universe has come about due to the failure of various cosmological models to correctly predict the amount of large scale structure (voids and walls), or the observed peculiar velocities of the bright galaxies. Parallel to these efforts was the suggestion from grand unified theory (GUT) of new types of stable particles with non-zero mass that interact only weakly with baryons (Turner 1987). The introduction of cold dark matter (CDM) resolves the following cosmological problems: 1) it allows Ω_o=1 without violating the baryon density (Ω_b=0.2) set by primordial nucleosynthesis, 2) CDM allows growth of present day large scale structure from fluctuations currently measured by COBE in the cosmic microwave background (CMB), since the CMB only responds to baryons, 3) CDM can be more smoothly distributed than baryons such that dynamical estimates for Ω_o are too low, 4) it resolves conflicts between cluster models and the galaxy distribution since galaxies do not trace the mass and 5) weak interactions form the basis to segregate baryonic and non-baryonic matter to form dark halos (see Oemler 1988 for a review). The only missing piece is a mechanism to segregate CDM from baryonic matter. On small scales, such as galaxy halos, dissipation is sufficient, but on large scales the mechanism remains undetermined. This has led to the speculation that an inefficiency in galaxy formation produces a bias in the distribution of bright galaxies such that they only trace the peaks of the mass distribution. The theoretical justification for biasing arises from the assumptions that if galaxies form from high σ fluctuations and if those fluctuations are superimposed on uncorrelated, random, larger-scale fluctuations of small amplitude, then galaxies will be more clustered than the underlying matter distribution (Kaiser 1984).

The theoretical community has also found support for a biased galaxy formation scheme in the many selection effects inherent in galaxy catalogs. Selection effects towards high mass galaxies that would maximize a biased interpretation from observational results such as the autocorrelation function for galaxies. For example, there is a clear surface brightness bias in galaxy catalogs to select against objects with central surface brightnesses near or below the natural sky brightness. Theory predicts that low surface brightness (LSB) galaxies are the result of lower amplitude fluctuations and that redshift surveys, without a complete sample of LSB objects, are biased (Mo, McGaugh and Bothun 1994). Although not all LSB galaxies are dwarfs (Bothun *et al.* 1987) nor are all dwarfs of a LSB nature (Loose and Thuan 1986), a majority of HI-rich dwarfs have central surface brightnesses below 23 B mag arcsec^{-2} (Schneider *et al.* 1990). Magnitude limited catalogs are known to be sparse in LSB galaxies (Sandage and Tammann 1981) and angular-limited catalogs, such as the UGC (Nilson 1973), that have deeper surface brightness levels will fail to find small dwarf galaxies at useful distances to study large scale structure since they quickly fall below the angular size limits for redshifts greater than 1000 km sec^{-1}. Searches for dwarf galaxies have primarily focused on nearby rich clusters, such as Virgo or Fornax (Sandage and Binggeli 1984, Caldwell and Bothun 1987), due to the vast number of objects located in a small region of the sky and with distances being determined by association with the cluster. But cluster catalogs are not

useful in studying the large scale distribution of dwarfs. Current all sky catalogs sample the less dense field population (e.g. the DDO catalog, van den Bergh 1960) and are rich in the lowest and faintest type of dwarfs, but are restricted to very local objects. The purpose of this project is to overcome these complimentary deficiencies in galaxy catalogs by attempting to recover field LSB dwarf galaxies through the use of Second Palomar Sky Survey plates.

In addition to the interest in the properties and content of dwarf galaxies with respect to global issues of galaxy formation and evolution, dwarf galaxies are also the leading candidates for the well known faint blue galaxies excess at moderate redshifts (FBE, see Kron 1980, Tyson 1988, Lilly, Cowie and Gardner 1991). Current models indicated that a majority of the FBE can be explained by a simple, evolving dwarf population (Driver *et al.* 1996). Estimates are that up to 30% of the galaxy luminosity density is due to dwarfs and the number density is 20 times greater than that of normal or giant galaxies. This population is typically low in mean surface brightness and fails to be included in catalogs based on isophotal magnitude or diameter. Thus, a secondary goal of this project is to investigate the optical and HI properties of a unbiased sample of dwarfs, selected by morphology and unrestricted by surface brightness. Papers II and III in this series will deal with these topics.

All distance related values in this paper use values of $H_o = 85$ km sec^{-1} Mpc^{-1}, $\Omega_o = 0.2$, a Virgo velocity of 977 km sec^{-1} and a Virgo infall of 300 km sec^{-1}.

2. A Search for Dwarf Galaxies

The key phase of this project was the identification of objects to test the biased galaxy formation hypothesis. For this test, the selection of a large sample of low mass or dwarf galaxies is required. There have also been recent arguments in the literature that low surface brightness galaxies are better test particles for biasing schemes (see Mo, McGaugh and Bothun 1994). In either case, the current catalogs which contain a suitable number of objects, such as the DDO (van den Bergh 1960) or the UGC (Nilson 1973), have insufficient depth in redshift space to sample a significant number of either dwarf or LSB galaxies.

A search for dwarf galaxies has one advantage over other catalog work; the unique morphology of dwarf galaxies makes them easily recognizable even at large distances. Dwarf galaxies come in two general morphological types, dwarf ellipticals (dE) and dwarf irregulars (dI), basically reflecting symmetry in their isophotes. The dwarf ellipticals, although having the same symmetry as giant ellipticals, differ in their intrinsic profile shapes having exponential rather than power-law distributions. This produces a diffuse appearance for dE's on photographic plate material which easily separates them from background normal ellipticals (see discussion in Binggeli, Sandage and Tammann 1985). Dwarf irregulars range from the extremely high surface brightness blue compact dwarfs (BCD's) to the very faint Virgo irregulars (see Sandage and Binggeli 1984). However, despite the range in mean surface brightness, their chaotic appearance distinguishes them from every

other Hubble type.

As shown in Schombert *et al.* (1992), a catalog of LSB galaxies is composed primarily of three classes of objects; 1) dwarfs, 2) LSB disks (quiescent counterparts of late-type star-forming spirals) and 3) Malin objects (supergiant LSB disks). To avoid the latter two categories in our sample, we concentrated our follow-up observations on objects that appeared to be Sm, Im, Irr, BCD, dI or dE, with a special emphasis on LSB objects and objects with small (down to 20 arcsecs) angular size. We have followed the prescription for morphological classification as outlined in Sandage and Binggeli (1984) from the Virgo Cluster catalog. Although our sample is a field sample, there is no indication that field irregulars differ in morphological types from cluster irregulars.

A smaller angular size for this study, as compared to previous LSB catalogs from PSS-II plates, is key to the investigation of large scale structure. For comparison, the UGC, with its one arcmin size limit, would catalog objects 4 kpc in diameter out to only 1200 km sec^{-1}. Our visual search produced 310 candidates off of 35 plates (1400 square degrees). After eliminating duplication from objects in the overlap regions between plates, or objects that already exist on other catalogs, produced a final sample of 278 objects listed in Table 1. Six objects are shown in Figure 1, displaying the range in surface brightness and absolute luminosity that the sample entailed.

3. Observations

The Second Palomar Sky Survey (PSS-II, see Reid *et al.* 1991) provided all the plate material for this project. The PSS-II differed from the original sky survey in three important ways. The first is that the exposures were made in the latest Kodak IIIa plates, which have greater resolution and depth than the original surveys 103a emulsions (250 lines mm^{-1} versus 80 lines mm^{-1}). The smaller grain sizes of the IIIa emulsions, combined with modern hypersensitization techniques, also results in greater sky density and higher uniformity in the plate background which is critical in the detection of low surface brightness objects such as dwarf galaxies.

The second difference is that the 48-inch Oschin Schmidt on Palomar Mountain was significantly modified with a new corrector, an updated mirror support system and improved plate holders. The original corrector lens was replaced in 1985 with a achromatic plate constructed of Schott LLF6 and O'Hara BK7W. The resulting image sizes were better than 0.5 arcsecs for in focus point sources. However, the new corrector has a significant astigmatic component that required the construction of higher precision plate holders. These new plate holders are capable of bending a 1 mm glass plate of 14 inches in length to an accuracy of $\pm$ 15 μm and reduce the astigmatism to less than the typical seeing disk over the entire field of view.

The third difference between the old survey and PSS-II is that the spacing of the survey fields was decreased from 6 degrees to 5 degrees. This results in a greater overlay zone on each plate and provides a greater total plate area to confirm the reality of detected objects. During this survey,

all objects in the overlap fields were independently confirmed in the neighboring plates.

The plates used for this project are A or B grade, selected for good surface brightness depth and covering declination zones of the sky that can be observed with the 305m Arecibo radio telescope. Plates with a grade of A are accepted for survey production having excellent uniformity and depth as well as prefect image quality. Plates with a grade of B are rejected for survey production for cosmetic reasons (aircraft or satellite trails, mild stellar elongation at the plates edges). B grade plates have the same depth and uniformity as A grade plates and the differences are irrelevant for this project. Due to the limited declination range of the Arecibo facility, and the incomplete status of the Second Sky Survey, only 35 fields were examined. All the plate inspection was accomplished by one of us (JMS) over a period of four months.

The inspection procedure consisted of marking the plate in 1 square degree regions and using a low power eyepiece to search and mark candidate objects. The identity of each marked object was cross-correlated to known galaxies using the POSS transparencies. The plate scales remained the same between the old and new survey and the transparencies contain all the objects from the NGC, IC, UGC and CGCG catalogs, as well as the Arp and Markarian lists. The coordinates of each candidate dwarf were taken directly from the plate material using a fine ruler and the position of SAO stars. Accuracy of the coordinates were typically ±15 arcsecs based on the centering of the optical imaging, which is sufficient for detection with the Arecibo beam of 3 arcmin diameter.

We observed the dwarf candidates in our list for the HI line at 21 cm with the Arecibo 305m telescope during the 1992 and 1993 observing season. All observations were made with the 21 cm dual-circular feed positioned to provide a maximum gain (8 K Jy^{-1}) at 1400 MHz. The 2048 channel autocorrelator was used and the independent, opposite polarized signals were each divided into two subcorrelators of 512 channels. In order to search a larger velocity space, the secondary local oscillators of each polarization set of subcorrelators were offset on either side of the standard local oscillator frequency of 260 MHz by 8.75 MHz, allowing a total velocity coverage of 8000 km s^{-1}, a velocity resolution of 8.6 km s^{-1}, and some overlap at the band edges. The observations were centered on 4000 km s^{-1}, which avoided detection of the strong Galactic hydrogen signal on the low-velocity end, and extended to 8120 km s^{-1}. Observations were made in the total power mode with 5 minute ON- source and OFF-source observations. In most cases, only one 5-minute ON-source integration was required for detection. Wherever possible, the zenith angle was kept less than 14 degrees to minimize the degradation of the gain. Details of the HI observations and analysis will be presented in an upcoming paper (Eder *et al.* 1997).

Successful detections were later selected for follow-up CCD imaging on the Hiltner 2.4m telescope located at Michigan-Dartmouth-M.I.T. (MDM) Observatory. We obtained images using either a Thomson 400 $\times$ 576 pixel CCD (0.25 arcsec pixel^{-1}) or a Ford-Loral 2048 $\times$ 2048 pixel CCD binned 3$\times$3 (0.51 arcsec pixel^{-1}), with minimal exposure times of 25 minutes in Johnson V and 15 minutes in Johnson I. Details of the optical observations and analysis will be presented in an upcoming paper (Pildis *et al.* 1997).

4. Discussion

From our initial sample of 310 objects, 277 with high quality indices were observed on the Arecibo 300m telescope at 21-cm out to a velocity of 10,000 km $\sec^{-1}$. Of the galaxies observed, 145 were detected. The objects not detected were probably background LSB spirals (with spiral patterns that were not visible on the plates) or gas-poor dwarfs (dE's). The loss of gas-poor dwarfs from the sample is unfortunate since the distribution of dE's outside of a cluster environment is not known or even if a true dE exists independent of a high local density or nearby companion (Binggeli, Tarenghi and Sandage 1990). However, it is not critical to our attempt to locate low mass test particles at cosmologically interesting distances. The catalog of objects are listed in Table 1 with the object name in column 1, object coordinates (1950) in column 2, heliocentric velocity from HI detections in column 3, morphological type in column 4 and any notes or comments in column 5. Images of all HI detected objects can be found at http://zebu.uoregon.edu/∼js/dwarf.html.

One of the first issues concerning the catalog was whether it is an accurate locator of dwarf galaxies. The original concept of dwarf galaxy was derived from the identification of small, faint companions to normal galaxies such as M32 and the dwarfs around M82. Later schemes emphasized their unique morphology (irregular), star formation histories and their impact on galaxy formation theory (see Binggeli 1993 for a review). Since most dwarf galaxies were faint in luminosity and surface brightness, it was not too surprising to find these observables reflected in similar physical attributes, i.e. dwarf galaxies are low in mass and mass surface density. Low mass and density imply an origin in low amplitude fluctuations in the early Universe and, thus, this study's interest in them as test particles. This does not diminish intrinsic interest in their properties since, after a short inspection of any dwarf catalog, it is obvious that their smaller mass and densities has produced dramatically different star formation histories as compared to giant or normal galaxies.

In order to understand the results of a morphologically selected sample, and test whether a true sample of dwarf galaxies has been selected by this catalog, we compare the properties of our catalog objects to dwarf samples in the literature (Schneider *et al.* 1990) and the properties of the UGC catalog (Nilson 1973, Huchtmeier and Richter 1989). The optical and HI data for this comparison is presented graphically here, but will be published in our companion papers. The reader should note that a HI detection is required for any absolute magnitude or scale length comparison since the only source of redshift information is at 21-cm. Optical redshifts would be very telescope time intensive due to the LSB nature of the sample and that time was better used in photometry portion of the project. Therefore, the following analysis is based on a HI-selected dwarf sample and by necessity avoids gas-poor dwarfs (e.g. dE's).

A first order definition of the difference between a dwarf galaxy and a normal or giant galaxy would focus on a comparison of masses. Historically, mass is not a directly determined quantity in galaxies and, thus, luminosity is used since the range of mass-to-light of giant galaxies for a given Hubble type is quite small due to simple past histories of star formation. However, a division between dwarf and giant galaxies by luminosity distorts the vast range of current star formation

rates in dwarf galaxies. For example, it is also possible for dwarf galaxies to have relatively high luminosities (e.g. A1212+06, a BCD in the Virgo cluster).

The luminosities of our sample galaxies and other optical properties are shown in Figure 2. The optical data will be presented and further discussed in Pildis *et al.* 1997, however, several trends are worth noting here. The total luminosities for the sample are, as expected, low with most of the galaxies having $M_V > -18$ mags. The central surface brightnesses are also low with a typical value between 21 and 23 I mags arcsec^{-2} (approximately 22.5 to 24.5 B mags arcsec^{-2}). For comparison, the value of a Freeman disk is 21.65 B mags arcsec^{-2}. The scale length from exponential fits are typically less than 2 kpc (a normal disk galaxy has scale length around 3 kpc, de Jong 1996). Lastly, the mean colors of the sample are quite blue ($V - I$ between 0.5 and 1.0), but this is typical for LSB galaxies (Schombert *et al.* 1992, McGaugh 1992) regardless of dwarf or non-dwarf classification.

As noted above, the luminosity of a galaxy is sharply dependent on the recent star formation history. On the other hand, separation by scale size rather than luminosity has been shown to more closely follow underlying physical properties of a galaxy (De Jong 1996). With respect to isophotal metric size, this sample of morphological selected objects is also well below the mean of any other galaxy catalog. Figure 3 displays the distribution of isophotal sizes for our sample of dwarfs and the general distribution from galaxies in the UGC catalog with HI detections (UGC HI, Huchtmeier and Richter 1989, i.e. a comparison of HI selected samples). The isophotal size, R_{25}, is the metric radius at the 25 I mag arcsecs^{-2} isophote measured directly from surface brightness profiles of the dwarf galaxies. This is equivalent to the UGC diameters which are determined from isophotal levels that are approximately 26.5 B mag arcsecs^{-2}, the so-called Holmberg radius (most LSB objects have $B - I$=1.5 colors). Figure 3 also demonstrates that this sample is composed of objects with radii in the lower 25% of the distribution of UGC radii. The mean R_{25} value for UGC HI selected objects is 15 kpc, versus a mean radius of 4 kpc for our dwarf sample.

There are two additional methods for dividing a LSB sample into dwarfs and giants: HI mass and HI profile velocity width. HI mass is a direct measure of the gas mass in a galaxy, assuming that the molecular material is a constant fraction of the total gas mass. For disk galaxies, there is a fairly good correlation between gas mass and total mass of a galaxy (see Giovanelli and Haynes 1988). However, this relationship does not exist for dwarf galaxies, probably due to the nature of star formation in dwarf galaxies which can quickly consume large fractions of the gas reserves. In addition, due to their weak gravitational potential, star formation and gas heating is much more effective at removing gas from dwarf galaxies as compared to their giant galaxy counterparts. Thus, the ratio of gas to total mass is more dependent on a dwarf galaxy's past star formation history than its initial physical characteristics.

The distribution of HI masses is shown in Figure 4. Also shown in Figure 4 is the distribution of HI masses from the Schneider *et al.* (1990) study of UGC dwarfs and the general distribution of HI masses for all UGC galaxies regardless of morphological type (Huchtmeier and Richter 1989, all

corrected to $H_o = 85$). Our sample of morphologically selected objects matches closely the same range of HI masses as the UGC dwarfs. Both dwarf samples lie on the lower mass range of the UGC HI sample with masses less than log $M_{HI} = 9.5$. The mean UGC HI mass is log $M_{HI} = 9.7$. Interestingly, both the Schneider *et al.* (1990) and PSS-II samples have identical cutoffs at log $M_{HI} = 9.2$ to the point where an operational definition of a dwarf galaxy is one with an HI mass less than this value (bright elliptical galaxies being a clear violation of this criteria). Given the expected decoupling of HI mass to total mass (see discussion above), the results presented in Figure 4 is surprising. We believe that the strongest statement Figure 4 can demonstrate is to show that a morphologically selected sample of dwarfs (this study and the UGC dwarf sample) will yield similar distributions of HI masses.

The HI line profile width is a good tool for determining the mass of disk galaxies, but is less effective with dwarf galaxies since they are not completely rotationally supported and probably have a significant component of their velocity width due to bulk stellar motions. For an excellent discussion of converting HI profiles to total mass estimates see Staveley-Smith, Davies and Kinman (1992). For our needs it is sufficient to plot the distribution of HI profile widths as a check on the lack of high width objects in the sample. This plot is shown in Figure 5 with comparison data from the Schneider *et al.* (1990) and UGC HI sample. As in Figure 4, the dwarf samples are composed of the lowest width objects as compared to the total HI sample of galaxies in the UGC. The PSS-II dwarf sample has a slightly lower distribution of profile widths compared to the Schneider *et al.* (1990) dwarf sample, but this may be due to a selection effect to detect face-on LSB objects in a visual survey which, in turn, emphasizes the non-rotational component to the velocity profile. Only six of the detected PSS-II dwarfs displayed a double-horned HI profile indicative of a disk system. All six also displayed disk and bulge morphology and spiral features with inspection by deep CCD images. These six objects were latter classified as a new type of galaxy, dwarf spirals, and described in a previous paper (Schombert *et al.* 1995).

5. Results

A sample of isolated dwarf galaxies has been selected from PSS-II plates. The candidates are selected by morphological criteria and then confirmed with HI detection. We show that a sample selected in this fashion yields an excellent set of isolated dwarf galaxies, (i.e. not companions to bright galaxies), and our plots and discussion in the previous section demonstrate that morphologically selected candidates yield a sample dwarfs, as defined by optical or HI properties.

The redshift distribution of the catalog lies between 500 and 10,000 km sec^{-1}, making it a more useful map of large scale structure than previous dwarf catalogs. Our primary result is shown in Figure 6, the redshift cone plot of our dwarf sample as compared to the distribution of galaxies from the CfA Redshift Survey (ZCAT, see Marzke, Huchra and Geller 1994) and the UGC HI sample. The ZCAT and UGC samples are selected from the declination zones +5 to +25°.

The ZCAT sample was selected for bright galaxies (likely to be higher mass objects, a test of biased gaalxy formation). The UGC HI sample was selected to compare our HI dwarf sample's redshift distribution with another HI selected sample. Neither the ZCAT nor the UGC HI distribution is visually any different from the redshift distribution of our dwarf galaxies, in conflict with the predictions of biased galaxy formation theory. A full analysis of the data will be presented in the latter papers of our series.

We wish to thank the generous support of the University of Michigan and the Michigan-Dartmouth-M.I.T Observatory in carrying out the photometry portion of this program and Arecibo Observatory for the allocation of time to search for HI emission from the candidate dwarf galaxies. The research described herein was carried out by the Jet Propulsion Laboratory, California Institute of Technology, under a contract with the National Aeronautics and Space Administration. This work is based on photographic plates obtained at the Palomar Observatory 48-inch Oschin Telescope for the Second Palomar Observatory Sky Survey which was funded by the Eastman Kodak Company, the National Geographic Society, the Samuel Oschin Foundation, the Alfred Sloan Foundation, the National Science Foundation grants AST 84-08225 and AST 87-18465, and the National Aeronautics and Space Administration grants NGL 05002140 and NAGW 1710. R.A.P. was partially supported by a National Science Foundation Graduate Fellowship. This research has made use of the NASA/IPAC Extragalactic Database (NED) which is operated by the Jet Propulsion Laboratory, California Institute of Technology, under contract with the National Aeronautics and Space Administration.

REFERENCES

van den Bergh, S. 1960, ApJ, 131, 215.

Binggeli, B. 1993, *Panchromatic View of Galaxies*, eds: Hensler, Theis and Gallagher, Kiel, Germany.

Binggeli, B., Sandage, A. and Tammann, G. 1985, AJ, 90, 1681.

Caldwell, N. and Bothun, G. 1987, AJ, 94, 1126.

Davis, M. and Djorgovski, S. 1985, 1985, ApJ, 299, 15.

Dekel, A. and Rees, M. 1987, Nature, 326, 455.

Driver, S., Couch, W., Phillipps, S. and Windhorst, R. 1996, preprint.

Giovanelli, R., Haynes, M. and Chincarini, G. 1986, ApJ, 300, 77.

Giovanelli, R. and Haynes, M. 1988, *Galactic and Extragalactic Radio Astronomy*, (New York: Springer-Verlag), p. 522.

Huchtmeier, W. and Richter, O. 1989, *General Catalog of HI Observations of Galaxies*, (Berlin:Springer).

Kron, R. 1980, ApJ, 43, 305.

de Jong, R. 1996, Astron. Astrophysics, submitted.

Lilly, S., Cowie, L. and Gardner, J. 1991, ApJ, 269, 79.

Loose, H. and Thuan, T. 1986, *Mitteil. Astron. Gesellschaft*, 65, 231.

Marzke, R., Huchra, J. and Geller, M. 1994, ApJ, 428, 43.

McGaugh, S. 1992, Ph.D. thesis, Univ. of Michigan.

Nilson, P. 1973, Uppsala General Catalog of Galaxies, (Uppsala, Sweden: Societatis Scientiarum Upsaliensis).

Oemler, A. 1988, *Minnesota Lectures on Cluster of Galaxies and Large-Scale Structure*, (San Francisco: Astronomical Society of the Pacific), p. 19.

Sandage, A. and Binggeli, B. 1984, AJ, 89, 919.

Sandage, A. and Tammann, G. 1981, *A Revised Shapley-Ames Catalog of Bright Galaxies*, Carnegie Institution of Washington Publication No. 635, (Carnegie Institution of Washington, Washington, D.C.).

Schneider, S., Thuan, T., Magri, C. and Wadiak, J. 1990 ApJS, 72, 245.

Schombert, J., Pildis, R., Eder, J. and Oemler, A. 1995, AJ, 110, 2067. 1992, AJ, 103, 1107.

Schombert, J., Bothun, G., Schneider, S. and McGaugh, S. 1992, AJ, 103, 1107.

Staveley-Smith, L., Davies, R. and Kinman, T. MNRAS, 258, 334.

Tyson, A. 1988, AJ, 96, 1.

This preprint was prepared with the AAS LaTeX macros v4.0.

Fig. 1.— CCD images for six dwarfs from our catalog. North is at the top, East to the left. Each frame is 8 kpc on a side. Images of all the HI detected dwarfs are available on the Dwarf Galaxy Survey homepage (http://zebu.uoregon.edu/∼js/dwarf.html).

Fig. 2.— The optical properties of the HI detected dwarf galaxies are shown (data from Pildis *et al.* 1997). The optical properties are similar to previous dwarf samples being low in luminosity, small in scale length and faint in central surface brightness. The bluer $B-I$ colors (a typical elliptical has a $B-I$=1.5) is common for LSB galaxies (Schombert *et al.* 1992).

Fig. 3.— The distribution of isophotal radii (radius at 25.0 I mag arcsec^{-2}) are shown for our dwarf sample and the total HI UGC catalog for all Hubble types. The dwarf galaxies in this catalog are all less than 25% of the typical size for UGC objects.

Fig. 4.— The distribution of HI masses is shown for our dwarf sample, the UGC dwarf sample (Schneider *et al.* 1990) and the complete UGC sample. Our sample of morphologically selected objects matches closely the same range of HI masses as the UGC dwarfs. Both dwarf samples lie on the lower mass range of the UGC HI sample with masses less than log M_{HI} = 9.5. The mean UGC HI mass is log M_{HI} = 9.7.

Fig. 5.— The distribution of HI profile widths is shown for our dwarf sample, the UGC dwarf sample (Schneider *et al.* 1990) and the complete UGC sample. As in Figure 4, the dwarf samples are composed of the lowest width objects as compared the total HI sample of galaxies in the UGC.

Fig. 6.— The redshift cone plot of our dwarf sample as compared to the distribution of galaxies from the CfA Redshift Survey (ZCAT, see Marzke, Huchra and Geller 1994) and the UGC HI sample. The ZCAT and UGC samples are selected from the declination zones +5 to +25°. The ZCAT sample was selected for bright galaxies (likely to be higher mass objects). The UGC HI sample was selected to test for selection effects due to an HI selected sample. Neither distribution is visually any different from the redshift distribution of our dwarf galaxies, in conflict with the predictions of biased galaxy formation theory.

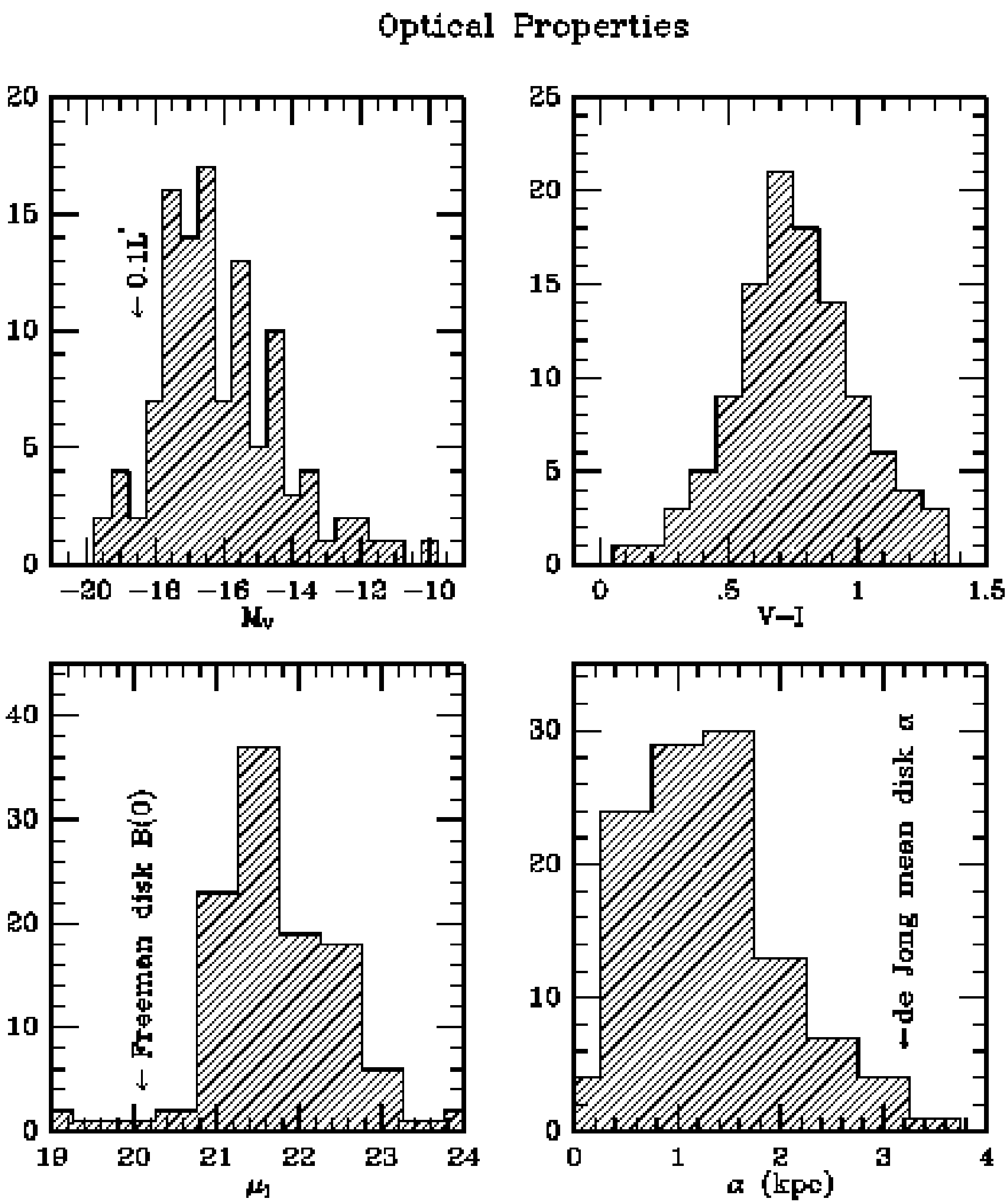
Optical Properties
← 0.1L*
M_V
V−I
← Freeman disk B(0)
μ_I
←de Jong mean disk α
α (kpc)

Figure 2

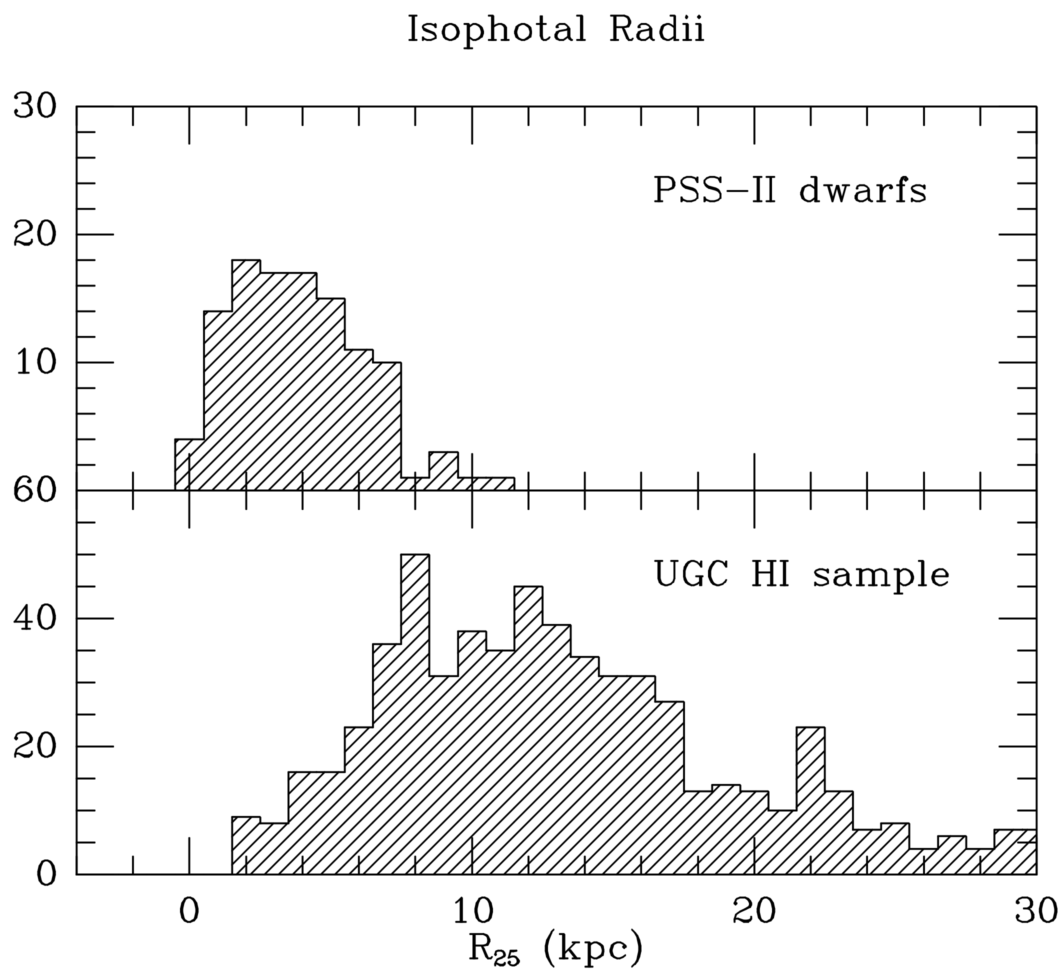
Isophotal Radii
PSS-II dwarfs
UGC HI sample
30
20
10
60
40
20
0
0
10
20
30
R_{25} (kpc)

Figure 3

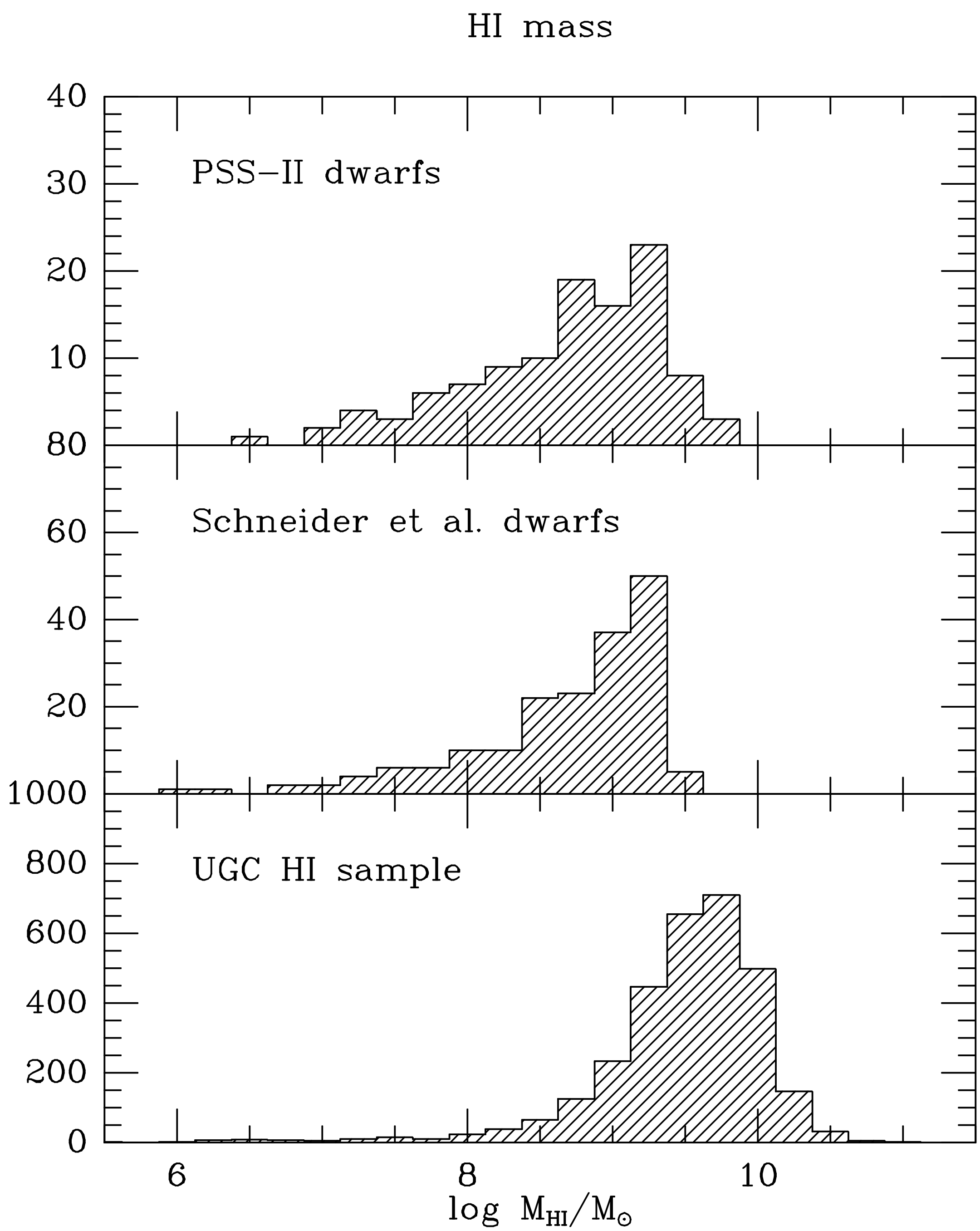
HI mass
PSS–II dwarfs
Schneider et al. dwarfs
UGC HI sample
40
30
20
10
80
60
40
20
1000
800
600
400
200
0
6
8
10
log $M_{HI}/M_{\odot}$

Figure 4

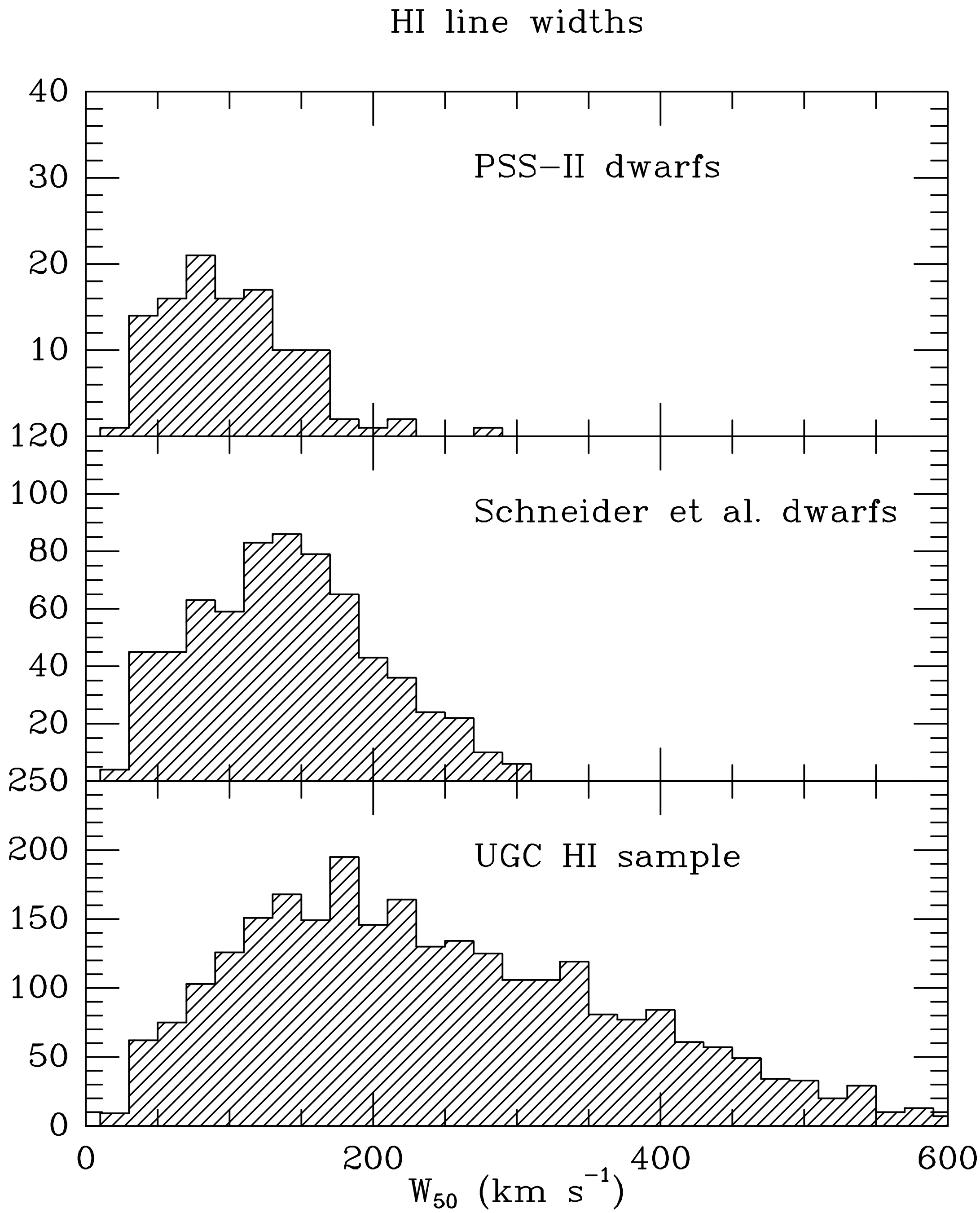
HI line widths
PSS–II dwarfs
Schneider et al. dwarfs
UGC HI sample
40
30
20
10
120
100
80
60
40
20
250
200
150
100
50
0
0
200
400
600
W50 (km s-1)

Figure 5

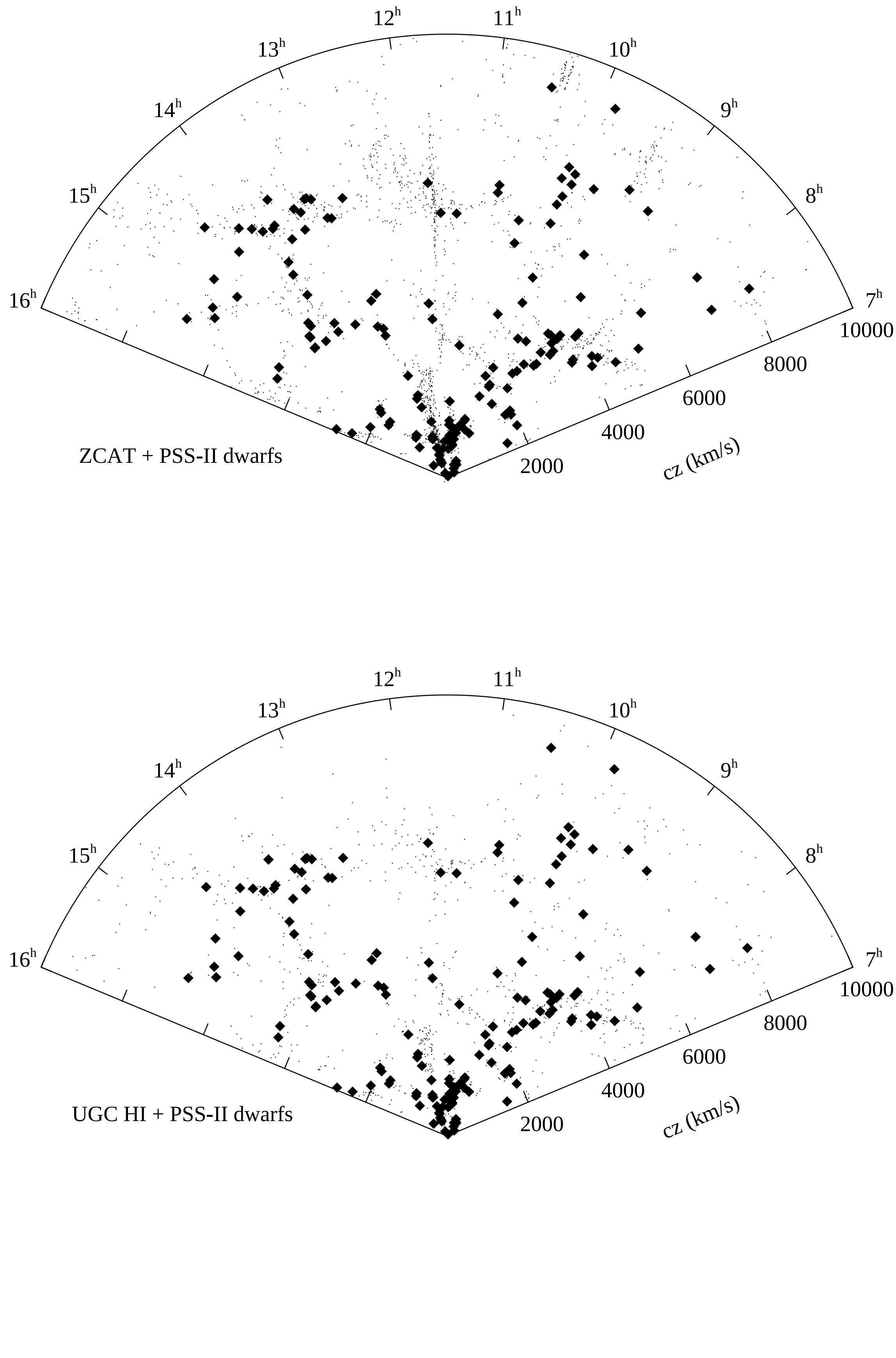
12h
11h
13h
10h
14h
9h
15h
8h
16h
7h
10000
8000
6000
4000
2000
cz (km/s)
ZCAT + PSS-II dwarfs
12h
11h
13h
10h
14h
9h
15h
8h
16h
7h
10000
8000
6000
4000
2000
cz (km/s)
UGC HI + PSS-II dwarfs